available at www.sciencedirect.com

ScienceDirect

www.elsevier.com/locate/brainres

BRAIN RESEARCH

Research Report

Regional differences in circadian period within the suprachiasmatic nucleus

Takako Noguchi[1], *Kazuto Watanabe**

Department of Regulatory Physiology, Dokkyo Medical University School of Medicine, 880 Kitakobayashi, Mibu, Tochigi 321-0293, Japan

ARTICLE INFO

Article history:
Accepted 23 August 2008
Available online 9 September 2008

Keywords:
Circadian rhythm
Vasopressin
Suprachiasmatic nucleus
Synchronization
Vasoactive intestinal polypeptide

ABSTRACT

In mammals, circadian rhythms are driven by a pacemaker located in the suprachiasmatic nucleus (SCN), which is composed of multiple, single-cell oscillators. Isolated SCN tissue shows clear circadian oscillation in release of arginine vasopressin (AVP) in organotypic slice cultures. Previously, we reported that the oscillators in the dorsal SCN have shorter periods than those in the ventral part. Here, we examined whether a correlation between the period and the rostral–caudal co-ordination could exist. The rostral, central and caudal SCN were cultured separately and the periods of circadian rhythms of AVP release were measured. The rostral and caudal parts of the SCN showed shorter periods than the central SCN. Together with previous findings, it is suggested that the shorter period region originates from AVP containing areas, while the longer period region corresponds with vasoactive intestinal polypeptide (VIP) containing cells. In our VIP-immunoreactive slices, the application of VIP antagonists shortened the periods of the AVP-releasing rhythm. These data indicate that the oscillators in AVP cells have short periods and are entrained by VIP cells to form a single integrated rhythm.

1. Introduction

Most of behavioral and physiological processes such as sleep, food intake and hormone secretion show daily rhythms. These temporal variations are generated by the biological clock located in the suprachiasmatic nucleus (SCN) (Stephan and Zucker, 1972; Meijer and Rietveld, 1989). Single neurons in the SCN can work as oscillators that continue to generate about 24 h rhythms in electrical activity in dispersed cell cultures (Welsh et al., 1995; Liu et al., 1997; Honma et al., 1998). The molecular mechanism underlying cell-autonomous rhythm generation has been described as a negative transcription–translation-based feedback loop (Okamura et al., 2002).

The SCN is anatomically divided into two regions; ventrolateral SCN or "core" and dorsomedial SCN or "shell", which is predominantly composed of neurons containing vasoactive intestinal polypeptide (VIP) and arginine vasopressin (AVP), respectively (Moore et al., 2002). The circadian oscillators in these subdivision have different properties with respect to light-responsiveness and temporal patterns of gene expression. The light-responsive cells are located in the core where the fibers of retino-hypothalamic tract from retina terminate (Moore et al., 2002). The core and the shell show different temporal expression patterns of per1 and AVP mRNA in hamster (Hamada et al., 2004) and a different response to a shorter and longer photoperiod (Inagaki et al., 2007, Jagota et al., 2000). There are differences in the circadian phases of

* *Corresponding author*. Fax: +81 282 86 7835.
E-mail address: kazuto-w@dokkyomed.ac.jp (K. Watanabe).
[1] Present address: National Institute of Advanced Industrial Science and Technology (AIST) Cell Dynamics Research Group, Research Institute for Cell Engineering.

0006-8993/$ – see front matter © 2008 Elsevier B.V. All rights reserved.
doi:10.1016/j.brainres.2008.08.082

mper1 expression in individual SCN cells in a slice culture even when they are well synchronized (Yamaguchi et al., 2003, Quintero et al., 2003). The mper1 expression in the shell reaches its peak level earlier than in the core and they keep the same phase angle under constant conditions. Although the two subdivisions would synchronize each other to form a single integrated oscillator, the coupling mechanisms remain to be determined. Possible candidates of intercellular synchronization include gamma-aminobutyric acid (GABA), VIP, gastrin-releasing peptide (GRP), nitric oxide and glial communications (Meijer and Schwartz, 2003).

The periods of single oscillatory neurons in the SCN are broadly ranged from 20 h to 28 h (Welsh et al., 1995; Liu et al., 1997; Honma et al., 1998). However, it has not been examined to what extent period differences are related to the neuroanatomical characteristics of the cells or the location within the SCN. We previously reported that the period of AVP-releasing cell rhythm in the dorsal SCN is shorter than that in the ventral SCN (Noguchi et al., 2004). In this study, we examined the correlation between period length and the rostral–caudal position in the SCN.

2. Results

2.1. *Culture of the rostral and the caudal part of the SCN*

Three consecutive 300 μm coronal sections aimed to the SCN region were prepared from an animal and the slices were cultured separately. A robust AVP-releasing rhythm was observed in one of the slices as reported previously (Noguchi et al., 2004), and a rostral or caudal adjacent slice also showed detectable AVP-releasing rhythm in many cases. Usually, the rhythm was observed in two of three consecutive slices, namely, the SCN was divided into two, the large part of the SCN (the central SCN) and either the rostral or the caudal part of the SCN (Figs. 1A and B). The average amount of AVP release was 62.9±2.5 pg/d (mean±SEM, n=130) in central slices, 21.7±1.9 pg/d (n=39) and 21.9±1.9 pg/d (n=51) in rostral and caudal slices, respectively (Fig. 1C). The amount of AVP release indicates the approximate sizes of the SCN in the slices.

The phases of AVP rhythms in the rostral slices were slightly advanced from that in the central slices (Figs. 2A and B). The phase differences grew larger during several days in culture. The differences in phases between caudal and central slices were more remarkable (Figs. 2C and D). The results indicated that the caudal and rostral slices have shorter periods than the central slices. The mean period of central slices was 23.7±0.03 h (mean±SEM, n=130). The period of caudal slices (22.9±0.1 h; mean±SEM, n=51) was distinctly shorter than that of central slices. The difference in mean periods between rostral (23.4±0.1 h; mean±SEM, n=39) and central slices was small but statistically significant (Fig. 3A).

The correlation between the amount of AVP release and the periods was examined. Both the shorter periodic slices released less amount of AVP. Although the AVP release and periods showed a positive correlation in each case, the patterns of the scatter diagram were different among SCN subdivisions. In the caudal slices, the periods became shorter as the AVP release decreased (r=0.62, Spearman's correlation coefficient by rank test) (Fig. 3B). The correlation was less evident in central and rostral slices but they were significant (central, r=0.56; rostral, r=0.40; P<0.05, Pearson's correlation coefficient test). In previous study, we showed the dorsal SCN had the shorter period than the ventral SCN. The ventral SCN released less amount of AVP than the dorsal SCN, while they had the longer period than the dorsal SCN. The amount of AVP release was not correlated with the period in this case. Together with the former findings, the following explanation is rather likely; in the caudal or rostral slices, the amount of AVP release is an index of the approximate size of the SCN in the slice, and the low amount of AVP release means a large distance from the center of the SCN. The data would indicate that more rostral or more caudal slices have shorter periods. To study further, we examined the distribution of AVP cells and VIP cells in the SCN slice immunohistochemically.

2.2. *Immunohistochemical analysis of cultured SCN slices*

A part of the slices were double-immunolabelled for arginine vasopressin-associated neurophysin (NP-AVP) and VIP after the measurement of the AVP-releasing rhythm for 2 or 3 weeks. NP-AVP- and VIP-immunoreactive (-ir) areas in the SCN were quantitatively evaluated in three categorized slices,

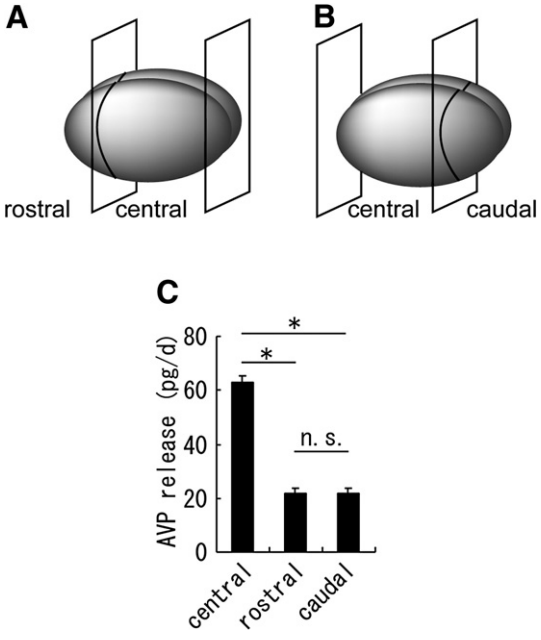

Fig. 1 – (A and B) Three consecutive 300 μm coronal sections aimed to the SCN region were prepared by a tissue chopper. Usually, the SCN was divided into two parts. The slice containing a large part of the SCN was categorized as a central slice and another slice adjacent to the central slice, containing a rostral or caudal tip of the SCN, was categorized as a rostral (A) or caudal slice (B), respectively. Gray oval objects indicate the SCN. Squares indicate cutting surface of slices. (C) The mean amount of AVP release from three categorized slices. Bars represent the mean±SEM. *P<0.01, Mann–Whitney's *U*-test with Bonferroni correction after Kruskal–Wallis *H*-test. n. s., no significant difference.

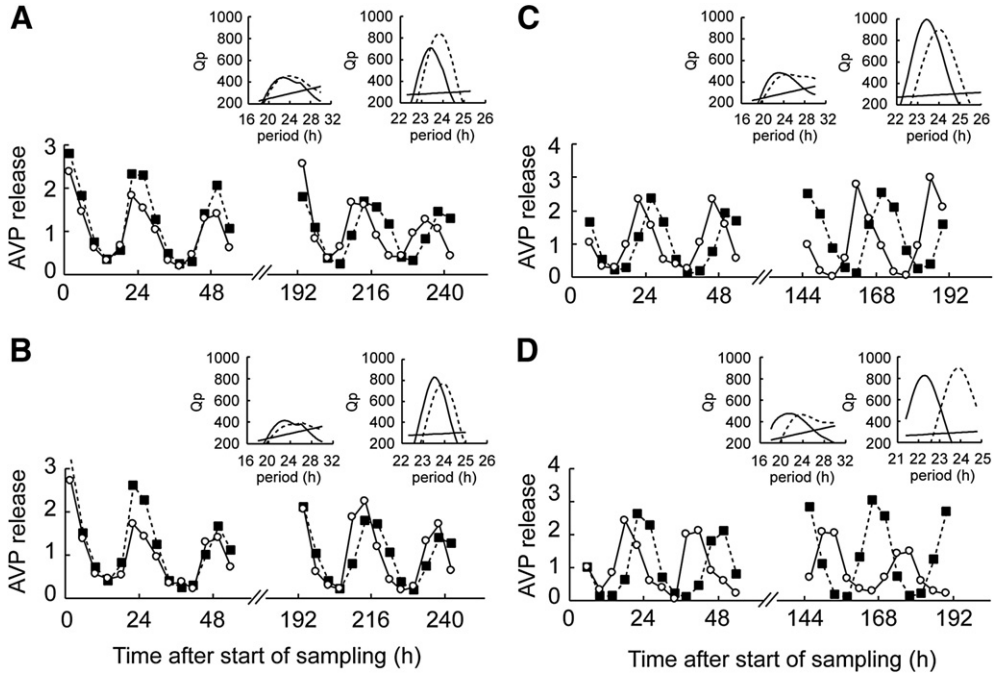

Fig. 2 – Circadian rhythm of AVP release in rostral, central and caudal slices. The slices were cultured for 1 week and the rhythm of AVP release was measured. AVP releases were plotted as a factor of the average value in an individual slice. The time after start of sampling was shown in *x*-axis. The AVP rhythm obtained from two adjacent SCN slices were compared. The results of central slices were shown by filled squares with dotted lines. The results of rostral (A and B) and caudal (C and D) slices were shown by open circles with solid lines. The inserts show the results of chi-square periodogram of each slice. The data of first half of the recording (left) or the combination of the first and the second half of the recording (right) was analyzed separately. Oblique lines represent a significant level of $P=0.01$.

rostral, caudal and central (Figs. 4A–I). The area of whole SCN is estimated from the nuclei stained by 4′, 6′-diamidino-2-phenylindole (DAPI). In central slices, the mean SCN area was $4.2\pm0.3\times10^5$ μm^2 (mean±SEM, $n=8$) (Fig. 4J). The cell density was 5.3 cells/1.0×10^3 μm^2 in 20 μm SCN section throughout the whole SCN. We could not find a regional difference in the cell density. The cell bodies which are strongly immunoreactive for NP-AVP were mainly found in the dorosomedial aspect of the SCN. NP-AVP-ir fibers are abundantly present in the ventral part of the SCN in many cases. As a result, NP-AVP-ir areas almost covered a whole SCN. Although AVP release into the medium was high at subjective day, we could not detect a large day–night difference in NP-AVP-ir areas (data not shown).

VIP-ir areas were present in about 40% of the whole SCN and were restricted to the ventral part. These distributions of neuropeptides in cultured SCN slices are consistent with former findings (Moore et al., 2002). In rostral and caudal slices, SCN areas were smaller than in central slices. In these slices, not only the SCN area but also proportions of VIP-ir areas to the whole SCN (VIP/SCN) were remarkably reduced (Fig. 4K). Notably, VIP-ir areas in caudal slices could not be found in some cases and the mean proportions to the whole SCN (8%) was much smaller than that of central slices. These results suggest that the VIP-ir cells are distributed to the central and ventral SCN and form a core of the SCN, on the other hand, NP-AVP-ir cells surround the core and form a shell of the SCN as reported previously (Moore et al., 2002).

We analyzed the correlation between periods and VIP/SCN over rostral, central and caudal slices. Interestingly, the periods become shorter as VIP/SCN ratios become lower (Fig. 5). The positive correlation including rostral, central and caudal slices was significant ($r=0.62$, $n=20$; Pearson's correlation coefficient test). These results indicate that the slices that contain smaller proportions of VIP-ir areas show shorter periods. It is possible that the period of AVP cells might be short and cells in VIP-rich region control the periods of the whole SCN.

2.3. *Inhibition of VIP-mediated synchronization*

To examine whether the core region controls the circadian oscillation of AVP cells by VIP or the other neurotransmitters, we tried to inhibit the intercellular VIP signaling using a VIP antagonist. The VIP antagonist (1 μM) was administered in central slices for 12 to 15 days continuously or with discontinuation during the sampling. The amount of the AVP release during the antagonist application was 41.1±6.2 pg/day (mean±SEM, $n=12$), which is slightly lower than that in control culture shown in Fig. 1C ($P<0.05$, Mann–Whitney *U*-test after Kruskal–Wallis *H*-test). The applications of the VIP antagonist shortened the periods of AVP-releasing rhythms (23.2±0.1 h, mean±SEM, $n=12$, $P<0.01$; Mann–Whitney's *U*-test with Bonferroni correction after Kruskal–Wallis *H*-test.) (Fig. 6A). The period was significantly shorter in comparison with that of control cultures. When the VIP

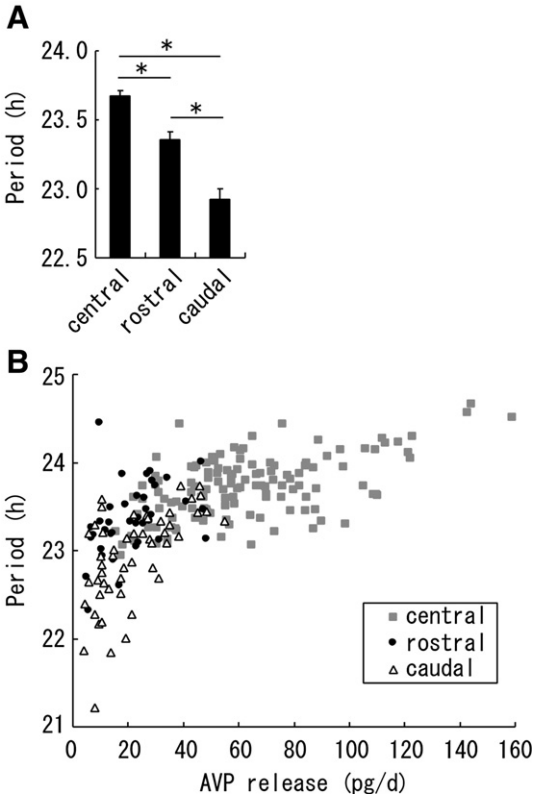

Fig. 3 – (A) Circadian period of AVP-releasing rhythm of central, rostral and caudal slices. The mean periods of these three SCN regions were significantly different each other. Bars represent the mean ± SEM. *P < 0.01, Student–Newman–Keuls test after Non-repeated Measures ANOVA. (B) Correlation between the amount of daily AVP release and periods. The results of central, rostral and caudal slices were shown by gray squares (■), filled circles (●) and open triangles (△), respectively.

antagonist was removed during the measurements of the rhythm, the effect of the antagonist disappeared (Fig. 6B). Continuous application of the VIP antagonist was necessary to shorten the periods of AVP rhythms. The effect of the VIP antagonist on periods was dose-dependent (Fig. 6D). The application of the VIP antagonist at 100 nM also shortened the period significantly.

3. Discussion

We have previously reported that the period of AVP-releasing rhythm in the dorsal SCN is shorter than that in the ventral SCN (Noguchi et al., 2004). In the present study, we showed that the periods of the rostral and caudal SCN were shorter than that of the central SCN. Actually, we compared the rhythm in a large slice (which contains the central SCN and either the rostral or caudal end) and a small slice (which contains another end of the SCN). The difference in period might come from the tissue size or the cell number of the SCN, but we believe this is not likely. As we have previously reported, there is no difference in period between the ventral half and the whole SCN (Noguchi et al., 2004). Furthermore, even when the right and left SCN were divided, their period did not change (data not shown). The difference in period became clear when the rostral or caudal slices were taken further from the center of the SCN. These results suggest that the shorter periodic region is located in the

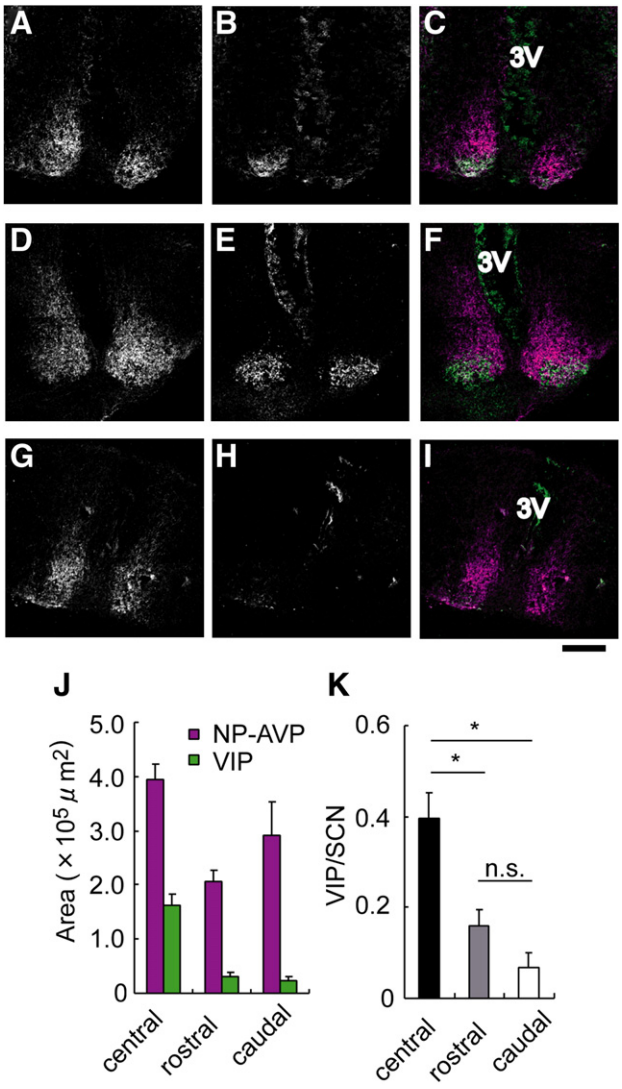

Fig. 4 – Immunohistochemical analysis of AVP-associated neurophysin (NP-AVP)- and vasoactive intestinal polypeptide (VIP)-immunoreactive (-ir) areas. The representative images of rostral (A–C), central (D–F) and caudal (G–I) slices were shown. NP-AVP-immunoreactivities are shown purple and VIP-immunoreactivities green. (A, D and G) NP-AVP-ir cells. NP-AVP-ir areas covered most of the SCN. (B, E and H) VIP-ir cells. VIP-ir areas were found in ventral SCN. Scale bar, 200 μm. (C, F and I) Merged images of NP-AVP- and VIP-ir areas. (J) Quantities of NP-AVP- and VIP-ir areas. NP-AVP- and VIP-ir areas were shown by purple and green bars, respectively. (K) Proportions of VIP-ir areas to the whole SCN (VIP/SCN) in central, rostral and caudal slices were shown. Bars represent the mean ± SEM. *P < 0.01, Mann–Whitney's *U*-test with Bonferroni correction after Kruskal–Wallis *H*-test. n. s., no significant difference. 3V, third ventricle.

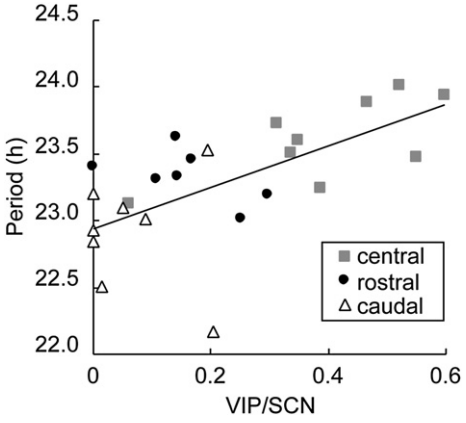

Fig. 5 – Correlation between periods and proportions of VIP-immunoreactive areas to the whole SCN (VIP/SCN). The results of central, rostral and caudal slices were shown by gray squares, filled circles and open triangles. The regression line obtained from a total of 20 data was shown ($P<0.01$, simple regression analysis). The period was positively correlated to VIP/SCN ($r=0.62$, Pearson's correlation coefficient test).

shell SCN and the region with longer periods of about 24 h is located in the core. Based on these data, we hypothesized that the shell SCN naturally has short periods and are entrained by the clocks in the core SCN to keep a normal period.

The immunohistochemical analysis showed that VIP cells are abundant in the centroventral SCN and the proportions of the VIP relative to the whole SCN (VIP/SCN) in a cross-section are smaller in rostral and caudal slices. Namely, VIP immunoreactivity is concentrated on the centroventral SCN and is lower in the rostral and caudal aspect. This localization of VIP is consistent with the observation in the adult rat SCN (Card et al., 1981). Interestingly, VIP/SCN in a slice was linearly correlated with the period of the slice. This result indicates that AVP cells can continue to oscillate with a normal period only when a sufficient number of pacemaker VIP cells are present in the slices. The application of a VIP antagonist, [Lys1, Pro2, 5, Arg3, 4, Tyr6]-VIP, shortened the periods of AVP release. The activity of this antagonist is validated in the sexual behavior of rats and in the single neuron activity in hypothalamic paraventricular nucleus (Gozes et al., 1989, Uchimura et al., 1996). This result further supports the hypothesis that the periods of AVP cells are short, and controlled by VIP cells. The application of a VIP antagonist with discontinuation had little effect on AVP-releasing rhythm. The results could be explained as follows: a VIP antagonist does not affect circadian oscillator machineries but inhibits the inter subdivisional communication between the core and shell. The shell runs fast according to its own period only in the presence of the antagonist. After removal of the antagonist, its oscillation is immediately synchronized to that of the core if the phase difference is small.

3.1. *Distinct functions of a core and shell*

A core and shell SCN have important distinctions in various aspects. The core contains VIP, GRP, GABA neurons and receives direct retinal input. The shell contains AVP, calretinin, GABA neurons and receives input from a core (Moore et al., 2002). Neurons in the core are light-responsive and express an immediate early-gene and clock genes, *per1* and *per2*, after a light pulse. The phase of *per1* expression in the shell is entrained by the core (Nagano et al., 2003, Nakamura et al., 2005). In the SCN slice culture using neonate rats, the AVP and VIP releasing rhythms can oscillate as if they are two independent oscillators (Shinohara et al., 1995, Nakamura et al., 2001). Combined measurement of AVP and VIP release would lead to further understanding of the relationship between the period and SCN subdivisions. However in our experiments, the VIP released in medium for a 4 h interval was

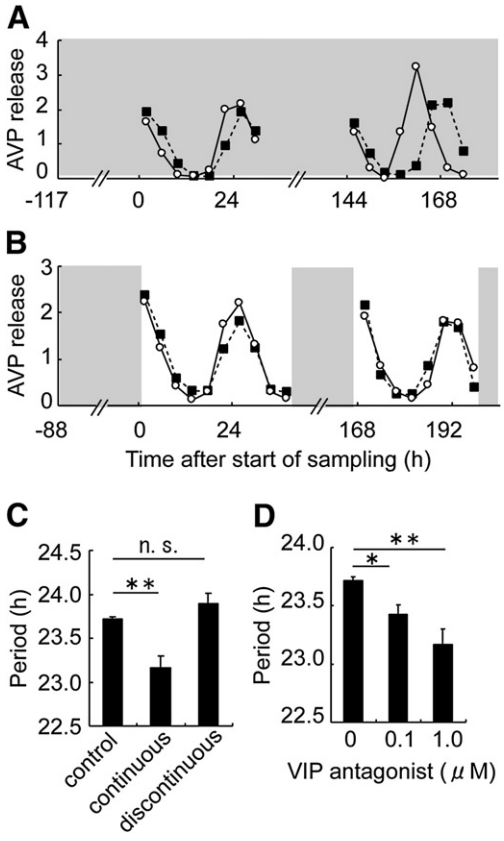

Fig. 6 – Circadian oscillation of AVP release in the presence of a VIP antagonist. To the cultures of the central slices, a 1 μM VIP antagonist was applied. AVP releases were plotted as a factor of the average value in an individual slice. The time after the start of sampling was shown in x-axis. The gray shadings show the period that the VIP antagonist was applied. The antagonist was continuously applied −117 h (117 h before sampling) to the end of sampling (A) or "−88 h to 0 h" and "40 h to 168 h" (with discontinuation during sampling) (B) (open circles with solid lines). The results without drug application were shown by filled square with dotted lines (A and B). (C) The effects of the VIP antagonist treatment on the periods. (D) Dose-dependency of the VIP antagonist applied continuously. Bars represent the mean ± SEM. $^{**}P<0.01$, $^{*}P<0.05$; Mann–Whitney's *U*-test with Bonferroni correction after Kruskal–Wallis *H*-test. n. s., no significant difference.

below the minimum detection level of a commercially available radio immunoassay kit. The present study suggested that these two functionally and anatomically different subdivisions have a difference in period and the period of the shell is entrained by the core.

3.2. *Coupling of core and shell*

The coupling of core and shell is necessary for generating synchronous rhythm within the SCN and the entrainment to external time cues. VIP is one of major candidates which mediates coupling between SCN neurons. The application of VIP phase-shifts the circadian rhythms similar to light, both *in vivo* and *in vitro* (Watanabe et al., 2000; Reed et al., 2001). The electrical activity rhythm in SCN slices was abolished by chronic treatment with a VIP antagonist, PG00-465 (Cutler et al., 2003). VIP and VIP receptor $VPAC_2$ deficient mice exhibit pronounced abnormalities in their response to light and synchronization among SCN neurons (Colwell et al., 2003; Aton et al., 2005). The locomotor activities of two thirds of these mutant mice were arrhythmic. However, one third of these mutant mice show a shortened period of wheel-running activity in constant darkness (Colwell et al., 2003; Aton et al., 2005). These results suggest the existence of VIP-independent short-period oscillators though they might be not dominant in generating the SCN rhythmicity. This result is consistent with our data that a VIP antagonist shortened the mean period of AVP-releasing rhythm. The other plausible intercellular synchronizing agent is GABA. GABA acting through A-type receptors, can affect the phase and synchrony of the clock cells (Liu and Reppert, 2000; Albus et al., 2005). It is also suggested that the GABAergic system is regulated by VIP (Colwell et al., 2003). However, the function of GABA has been controversial. Recent study showed that Gi/o, not GABA activity, converges with VIP signaling to maintain and coordinate rhythms among SCN neurons (Aton et al., 2006).

3.3. *Period determination in the SCN*

Single-cell recordings have revealed the presence of neurons with various periods, ranging from 20 to 28 h, and their mean period is about 24 h (Welsh et al., 1995; Liu et al., 1997; Honma et al., 1998; Herzog et al., 2004). The mean period of clock cells in culture is short in *tau* mutant hamsters, which have short behavioral periods and is long in heterozygous *Clock* mutant mice, which have lengthened behavioral periods (Liu et al., 1997; Herzog et al., 1998). Our recordings of single-cell firing rhythm have also shown that the period ranges from 21.5 h to 25.6 h (23.7±2.3 h, mean±SD) (unpublished data). When cells are dissociated and cultured at high density, however, they show one integrated AVP rhythm, and the variance in period among cultures is much smaller than that of a single-cell period (23.7±0.3 h) (Watanabe et al., 1995). The AVP rhythm of slice culture and high-density cell culture would be the results of the synchronization of individual cells. In the present and previous study, we found regional difference in the SCN; a shorter period in shell subdivision and a longer period in core subdivision. There was no subdivision which showed very short (<22.0 h) or very long (>24.5 h) periods The period of each subdivision might be the mean of the period in individual cells contained in the subdivision. However, there was no region with a longer period than that of whole SCN, which is close to that of behavioral rhythm. Thus, the period of the whole SCN was not the mean of the periods in each subdivision, but was equal to the longest period. In the cardiac pacemaker, the fastest pacemaker the sinoatrial node is responsible for the rhythm of whole heart's beat. All the other cells follow it in synchrony. However, a recent report on *Drosophila* circadian pacemakers showed an example which is against a "faster takes all" rule (Stoleru et al., 2005). It would be possible that there is a hierarchy among the individual oscillators and one oscillator is followed by the other oscillators regardless of their period.

Our present results suggest that neurons with different periods are organized in a core and shell. The period of AVP cells in a shell might be entrained by means of VIP. Defining the interaction of heterogeneous SCN cells is necessary to understand the circadian system as well as a regulatory system of clock genes.

4. Experimental procedures

4.1. *SCN slice culture*

The experiments were conducted using the Guidelines for the Care and Use of Laboratory Animals, Dokkyo University School of Medicine. We used 4–7 day-old rats (Sprague–Dawley) which were maintained on a 14:10-h light/dark cycle (light: 05:00–19:00). Slices were prepared as described previously (Noguchi and Watanabe, 2005). Briefly, the coronal sections (300 μm thick) of the brain were obtained using a tissue chopper (McIlwain, Surrey, England). Bilateral SCNs were trimmed to approximately 2×2 mm square. The slices were put on a 3 μm filter cup (Chemotaxicell, Kurabo, Osaka, Japan) and were placed in a 24-well culture dish. The slices on the filters were cultured with 400 μl Dulbecco's modified Eagle's medium supplemented with 10 mM HEPES (pH 7.4), 1.25 mg/ml NaHCO3, 100 μg/ml human transferrin (Sigma, St. Louis, MO, USA), 5 μg/ml insulin (Sigma), 100 μM putrescine (Sigma), 20 nM progesterone (Sigma), and 30 nM selenous acid. The cultures were maintained at 37 °C in a humidified air: CO^2 incubator (95%:5%).

To block the effect of intercellular communication by intrinsic VIP, a VIP antagonist ([Lys1, Pro2, 5, Arg3, 4, Tyr6]-vasoactive intestinal peptide human, porcine, rat) (Sigma) was applied to the culture. For continuous application, the antagonist was added to the medium at every medium change including the sampling. In some cultures, we omitted the application during the sampling (discontinuous application).

4.2. *Analysis of circadian rhythm*

To examine the presence of circadian rhythmicity, the medium was changed at 4 h intervals. The amount of AVP in the conditioned medium was measured by radioimmunoassay using ^{125}I-AVP (PerkinElmer, Boston, MA, USA) and specific antiserum (Watanabe et al., 1998). We measured AVP release for 7 to 10 days including a few days of discontinuation. The period of the rhythm was determined using a least square

spectrum method (Watanabe et al., 1995, Noguchi et al., 2004). Briefly, for a given period "τ", we obtained the best fitted cosine curve.

$$y(t) = M + A\cos(2\pi t/\tau + \varphi)$$

and calculated "p" value according to the following equation,

$$p = \left(\sum\left(y_i - y(t_i)^2\right)/\sum(y(t_i) - \hat{y})\right)^{(n-3)/2}$$

where "$\hat{y}$" is the average of y_i. And then we obtained optimum "τ" which gives a minimum "p" value. We also estimate the period by a chi-square periodogram in some cases (shown in Fig. 2 inserts). For this analysis, the original 4-h interval discrete data was converted to a continuous one by linear interpolation. As far as we examined, the difference between the values obtained by the periodogram and by the curve-fitting was less than 0.1 h.

4.3. *Immunohistochemistry of AVP and VIP areas in the SCN slice cultures*

The SCN slices were double-immunolabelled for NP-AVP and VIP after 2 or 3 weeks in culture. SCN slices with filter cups were fixed with 4% paraformaldehyde in 0.05 M phosphate buffer saline (PBS) overnight at 4 °C and incubated in 4% paraformaldehyde in 0.05 M PBS, 10% sucrose overnight at 4 °C. Then the filters with SCN slices were removed from cups. Following three 5 min rinses with PBS, the SCN slices with filter membranes were embedded in Tissue-Tek® O. T. C. compound (Sakura Finetechnical Co., Ltd., Tokyo, Japan). The slices were frozen on dry ice and transected using a cryostat into 20 μm thick sections, and mounted on MAS-coated micro slide glasses (Matunami Glass Ind., Ltd., Osaka, Japan). After removing the compound by three 5 min rinses with PBS, SCN sections were incubated in 5% normal goat serum, 1% Triton-X (Sigma), 0.02% azide in PBS (buffer G) for an hour at room temperature to block nonspecific antibody binding. The samples were incubated overnight at 4 °C with 1:200 monoclonal mouse antibody against NP-AVP, which is a generous gift from Dr. H. Gainer (NIH, Bethesda, MD), and rabbit anti-VIP serum (1:2000; Peptide Institute, Osaka, Japan) in buffer G. Following three 5 min rinses of the tissue with PBS, the samples were incubated with two secondary antibodies (1:400; Alexa Fluor® 594 donkey anti-mouse IgG and 1:800; Alexa Fluor® 488 donkey anti-rabbit IgG) (Molecular Probes, Eugene, OR, USA) overnight at 4 °C. After three 5 min rinses, the samples were sealed with SlowFade® Antifade Kit with DAPI (4′, 6′-diamidino-2-phenylindole) (Molecular Probes, Eugene, OR, USA).

4.4. *Quantitative analysis of AVP and VIP-immunoreactive areas*

The fluorescent image was viewed using a fluorescent microscope (ECLIPSE, Nikon, Tokyo, Japan) with an objective lens (Plan Fluor 10×/0.30, Nikon, Japan), a digital camera (DXM 1200F, Nikon, Tokyo, Japan). The digital images of NP-AVP- and VIP-immunofluorescence were processed to eliminate the background and leave the highly immunoreactive areas by Photoshop 7.0® (Adobe systems Inc., San Jose, CA, USA), respectively. The NP-AVP- and VIP-immunoreactive areas were surrounded by lines and quantified by Scion image (Scion Corporation, Frederick, MD, USA).

Acknowledgments

The authors would like to thank G.J. Boer and J.J. van Heerikhuize from the Netherlands Institute of Brain Research, Amsterdam, for the donation of anti-AVP antiserum; H. Gainer for the donation of the monoclonal mouse antibody against AVP-associated neurophysin; and J.H. Meijer for her critical reading of the manuscript. This work was supported by a Grant-in-Aid for scientific Research (No. 13670070 and no. 16590178) from Japan Society for the Promotion of Science to K.W. and by a Sasakawa Scientific Research Grant from The Japan Science Society to T.N.

REFERENCES

Albus, H., Vansteensel, M.J., Michel, S., Block, G.D., Meijer, J.H., 2005. A GABAergic mechanism is necessary for coupling dissociable ventral and dorsal regional oscillators within the circadian clock. Curr. Biol. 15, 886–893.

Aton, S.J., Colwell, C.S., Harmar, A.J., Waschek, J., Herzog, E.D., 2005. Vasoactive intestinal polypeptide mediates circadian rhythmicity and synchrony in mammalian clock neurons. Nat. Neurosci. 8, 476–483.

Aton, S.J., Huettner, J.E., Straume, M., Herzog, E.D., 2006. GABA and Gi/o differentially control circadian rhythms and synchrony in clock neurons. Proc. Natl. Acad. Sci. U. S. A. 103, 19188–19193.

Card, J.P., Brecha, N., Karten, H.J., Moore, R.Y., 1981. Immunocytochemical localization of vasoactive intestinal polypeptide-containing cells and processes in the suprachiasmatic nucleus of the rat: light and electron microscopic analysis. J. Neurosci. 1, 1289–1303.

Colwell, C.S., Michel, S., Itri, J., Rodriguez, W., Tam, J., Lelievre, V., Hu, Z., Liu, X., Waschek, J.A., 2003. Disrupted circadian rhythms in VIP- and PHI-deficient mice. Am. J. Physiol. Regul. Integr. Comp. Physiol. 285, R939–R949.

Cutler, D.J., Haraura, M., Reed, H.E., Shen, S., Sheward, W.J., Morrison, C.F., Marston, H.M., Harmar, A.J., Piggins, H.D., 2003. The mouse VPAC2 receptor confers suprachiasmatic nuclei cellular rhythmicity and responsiveness to vasoactive intestinal polypeptide in vitro. Eur. J. Neurosci. 17, 197–204.

Gozes, I., Meltzer, E., Rubinrout, S., Brenneman, D.E., Fridkin, M., 1989. Vasoactive intestinal peptide potentiates sexual behavior: inhibition by novel antagonist. Endocrinology 125, 2945–2949.

Hamada, T., Antle, M.C., Silver, R., 2004. Temporal and spatial expression patterns of canonical clock genes and clock-controlled genes in the suprachiasmatic nucleus. Eur. J. Neurosci. 19, 1741–1748.

Herzog, E.D., Takahashi, J.S., Block, G.D., 1998. Clock controls circadian period in isolated suprachiasmatic nucleus neurons. Nat. Neurosci. 1, 708–713.

Herzog, E.D., Aton, S.J., Numano, R., Sakaki, Y., Tei, H., 2004. Temporal precision in the mammalian circadian system: a reliable clock from less reliable neurons. J. Biol. Rhythms 19, 35–46.

Honma, S., Shirakawa, T., Katsuno, Y., Namihira, M., Honma, K., 1998. Circadian periods of single suprachiasmatic neurons in rats. Neurosci. Lett. 250, 157–160.

Inagaki, N., Honma, S., Ono, D., Tanahashi, Y., Honma, K., 2007. Separate oscillating cell groups in mouse suprachiasmatic nucleus couple photoperiodically to the onset and end of daily activity. Proc. Natl. Acad. Sci. U. S. A. 104, 7664–7669.

Jagota, A., de la Iglesia, H.O., Schwartz, W.J., 2000. Morning and evening circadian oscillations in the suprachiasmatic nucleus in vitro. Nat. Neurosci. 3, 372–376.

Liu, C., Reppert, S.M., 2000. GABA synchronizes clock cells within the suprachiasmatic circadian clock. Neuron 25, 123–128.

Liu, C., Weaver, D.R., Strogatz, S.H., Reppert, S.M., 1997. Cellular construction of a circadian clock: period determination in the suprachiasmatic nuclei. Cell 91, 855–860.

Meijer, J.H., Rietveld, W.J., 1989. Neurophysiology of the suprachiasmatic circadian pacemaker in rodents. Physiol. Rev. 69, 671–707.

Meijer, J.H., Schwartz, W.J., 2003. In search of the pathways for light-induced pacemaker resetting in the suprachiasmatic nucleus. J. Biol. Rhythms 18, 235–249.

Moore, R.Y., Speh, J.C., Leak, R.K., 2002. Suprachiasmatic nucleus organization. Cell Tissue Res. 309, 89–98.

Nagano, M., Adachi, A., Nakahama, K., Nakamura, T., Tamada, M., Meyer-Bernstein, E., Sehgal, A., Shigeyoshi, Y., 2003. An abrupt shift in the day/night cycle causes desynchrony in the mammalian circadian center. J. Neurosci. 23, 6141–6151.

Nakamura, W., Honma, S., Shirakawa, T., Honma, K., 2001. Regional pacemakers composed of multiple oscillator neurons in the rat suprachiasmatic nucleus. Eur. J. Neurosci. 14, 666–674.

Nakamura, W., Yamazaki, S., Takasu, N.N., Mishima, K., Block, G.D., 2005. Differential response of Period 1 expression within the suprachiasmatic nucleus. J. Neurosci. 25, 5481–5487.

Noguchi, T., Watanabe, K., 2005. Tetrodotoxin resets the clock. Eur. J. Neurosci. 21, 3361–3367.

Noguchi, T., Watanabe, K., Ogura, A., Yamaoka, S., 2004. The clock in dorsal suprachiasmatic nucleus runs faster than that in ventral. Eur. J. Neurosci. 20, 3199–3202.

Okamura, H., Yamaguchi, S., Yagita, K., 2002. Molecular machinery of the circadian clock in mammals. Cell Tissue Res. 309, 47–56.

Quintero, J.E., Kuhlman, S.J., McMahon, D.G., 2003. The biological block nucleus: a multiphasic oscillator network regulated by light. J. Neurosci. 23, 8070–8076.

Reed, H.E., Meyer-Spasche, A., Cutler, D.J., Coen, C.W., Piggins, H.D., 2001. Vasoactive intestinal polypeptide (VIP) phase-shifts the rat suprachiasmatic nucleus clock in vitro. Eur. J. Neurosci. 13, 839–843.

Shinohara, K., Honma, S., Katsuno, Y., Abe, H., Honma, K., 1995. Two distinct oscillators in the rat suprachiasmatic nucleus in vitro. Proc. Natl. Acad. Sci. U. S. A. 92, 7396–7400.

Stephan, F.K., Zucker, I., 1972. Circadian rhythms in drinking behavior and locomotor activity of rats are eliminated by hypothalamic lesions. Proc. Natl. Acad. Sci. U. S. A. 69, 1583–1586.

Stoleru, D., Peng, Y., Nawathean, P., Rosbash, M., 2005. A resetting signal between *Drosophila* pacemakers synchronizes morning and evening activity. Nature 438, 238–242.

Uchimura, D., Katafuchi, T., Hori, T., Yanaihara, N., 1996. Facilitatory effects of pituitary adenylate cyclase activating polypeptide (PACAP) on neurons in the magnocellular portion of the rat hypothalamic paraventricular nucleus (PVN) in vitro. J. Neuroendocrinol. 8, 137–143.

Watanabe, K., Katagai, T., Ishida, N., Yamaoka, S., 1995. Anisomycin induces phase shifts of circadian pacemaker in primary cultures of rat suprachiasmatic nucleus. Brain Res. 684, 179–184.

Watanabe, K., Yamaoka, S., Vanecek, J., 1998. Melatonin inhibits spontaneous and VIP-induced vasopressin release from suprachiasmatic neurons. Brain Res. 801, 216–219.

Watanabe, K., Vanecek, J., Yamaoka, S., 2000. In vitro entrainment of the circadian rhythm of vasopressin-releasing cells in suprachiasmatic nucleus by vasoactive intestinal polypeptide. Brain Res. 877, 361–366.

Welsh, D.K., Logothetis, D.E., Meister, M., Reppert, S.M., 1995. Individual neurons dissociated from rat suprachiasmatic nucleus express independently phased circadian firing rhythms. Neuron 14, 697–706.

Yamaguchi, S., Isejima, H., Matsuo, T., Okura, R., Yagita, K., Kobayashi, M., Okamura, H., 2003. Synchronization of cellular clocks in the suprachiasmatic nucleus. Science 302, 1408–1412.